

# **SIMULTANEOUS MEASUREMENT OF VAPOROUS AND AEROSOLIZED THREATS BY ACTIVE OPEN PATH FTIR**

**Ram A. Hashmonay, Ravi M. Varma, Mark Modrak, and Robert H. Kagann**

ARCADIS

4914 Prospectus Drive, Suite F  
Durham, NC 27713

**Patrick D. Sullivan**

Air Force Research Laboratory  
139 Barnes Drive, Suite 2  
Tyndall AFB, Florida 32403 USA

## **ABSTRACT**

The Environmental Protection Agency's open-path Fourier transform infrared (OP-FTIR) activities include passive and active measurements in several stack and fugitive emission monitoring applications. Extensive research has been devoted during the past two years to evaluate and validate various OP-FTIR technologies for the identification and detection of toxic industrial compounds and chemical warfare agents, primarily in the gas phase. This paper emphasizes the superiority of the active OP-FTIR system over the passive system in detection levels and data quality, and disputes misconceptions that are generally well accepted for FTIR technologies. Additionally, a new approach for detection and identification of aerosolized threats using an active modulated OP-FTIR is described. Revisiting the use of active OP-FTIR techniques is recommended as recently many non-battlefield detection applications have emerged.

## **INTRODUCTION**

The United States Congress provided funding for the Environmental Protection Agency's (EPA) Office of Research and Development (ORD) to perform building protection and decontamination research. ORD subsequently formed the National Homeland Security Research Center (NHSRC) to perform this research as well as research relating to water systems security and risk assessment. As a part of the building protection research program, existing monitoring methods have been evaluated for applicability. Open-path Fourier transform infrared (OP-FTIR) measurements are being used in several EPA stack and fugitive emission monitoring activities. In the last two years, under NHSRC funding, extensive research has been devoted to evaluating various OP-FTIR technologies for the identification and detection of toxic industrial compounds (TICs) and chemical warfare agents (CWAs), primarily in the gas phase. We also present a

# Report Documentation Page

*Form Approved*  
*OMB No. 0704-0188*

Public reporting burden for the collection of information is estimated to average 1 hour per response, including the time for reviewing instructions, searching existing data sources, gathering and maintaining the data needed, and completing and reviewing the collection of information. Send comments regarding this burden estimate or any other aspect of this collection of information, including suggestions for reducing this burden, to Washington Headquarters Services, Directorate for Information Operations and Reports, 1215 Jefferson Davis Highway, Suite 1204, Arlington VA 22202-4302. Respondents should be aware that notwithstanding any other provision of law, no person shall be subject to a penalty for failing to comply with a collection of information if it does not display a currently valid OMB control number.

1. REPORT DATE <b>15 NOV 2004</b>	2. REPORT TYPE <b>N/A</b>	3. DATES COVERED -			
4. TITLE AND SUBTITLE <b>Simultaneous Measurement Of Vaporous And Aerosolized Threats By Active Open Path Ftir</b>		5a. CONTRACT NUMBER			
		5b. GRANT NUMBER			
		5c. PROGRAM ELEMENT NUMBER			
6. AUTHOR(S)		5d. PROJECT NUMBER			
		5e. TASK NUMBER			
		5f. WORK UNIT NUMBER			
7. PERFORMING ORGANIZATION NAME(S) AND ADDRESS(ES) <b>ARCADIS 4914 Prospectus Drive, Suite F Durham, NC 27713</b>		8. PERFORMING ORGANIZATION REPORT NUMBER			
9. SPONSORING/MONITORING AGENCY NAME(S) AND ADDRESS(ES)		10. SPONSOR/MONITOR'S ACRONYM(S)			
		11. SPONSOR/MONITOR'S REPORT NUMBER(S)			
12. DISTRIBUTION/AVAILABILITY STATEMENT <b>Approved for public release, distribution unlimited</b>					
13. SUPPLEMENTARY NOTES <b>See also ADM001849, 2004 Scientific Conference on Chemical and Biological Defense Research. Held in Hunt Valley, Maryland on 15-17 November 2004 . , The original document contains color images.</b>					
14. ABSTRACT					
15. SUBJECT TERMS					
16. SECURITY CLASSIFICATION OF:			17. LIMITATION OF ABSTRACT <b>UU</b>	18. NUMBER OF PAGES <b>13</b>	19a. NAME OF RESPONSIBLE PERSON
a. REPORT <b>unclassified</b>	b. ABSTRACT <b>unclassified</b>	c. THIS PAGE <b>unclassified</b>			

unique method to simultaneously measure aerosol plumes such as spray field operations and pesticide drifts. In these and many other cases, the plumes are a mixture of aerosols and gases, similar to low-vapor-pressure CWAs. This measurement method is directly applicable for detection of low-vapor-pressure chemical agents.

Many of the CWAs and TICs exhibit strong infrared signals, which have led to an effort to adapt the current EPA practices to address applicable need of homeland security. In the past, the Department of Defense (DoD) required passive FTIR sensors as standoff techniques that did not need powered radiation sources or mirrors to detect CWAs in the battlefield. However, many recent military applications, like CWA stockpiles and force protection on permanent installations, do not necessarily merit passive standoff FTIR systems. And there is an enormous difference between the two types of FTIR configurations. In fact, the only element they share is the interferometer that gives the instrument its name. And yet, we found a lot of evidence that many potential users do not distinguish between active and passive methods when considering FTIR technology. The active OP-FTIR has much better detection capabilities and is far less prone to report false positive detections. Furthermore aerosol and gas-phase particles may be detected and identified only with a stable, modulated, active OP-FTIR instrument.

## 1. ACTIVE VS PASSIVE FTIR FOR VAPOR DETECTION

The schematics portrayed in Figure 1 illustrate the two possible configurations of active OP-FTIR systems: bistatic, in which the infrared radiation source and the detector are on the opposite sides of the beam path (upper diagram), and monostatic modulated, in which the source and the detector are on the same side (lower diagram) of the optical path. A passive configuration is similar to the bistatic configuration; however, it relies on natural surfaces that are only a few degrees different in temperature from the absorbing or emitting medium.

The monostatic configuration is more frequently used in emission monitoring applications, as it provides stable and sensitive concentration results. In this configuration the very hot radiation source (1500K) is modulated by the interferometer before the beam is transmitted out to the atmosphere. A corner-cube retroreflector is placed on the other side of the beam path to return the beam directly back to the detector. Such a configuration allows the cancellation of background radiation that may introduce noise and error to the measurement due to atmospheric temperature scintillation effects.

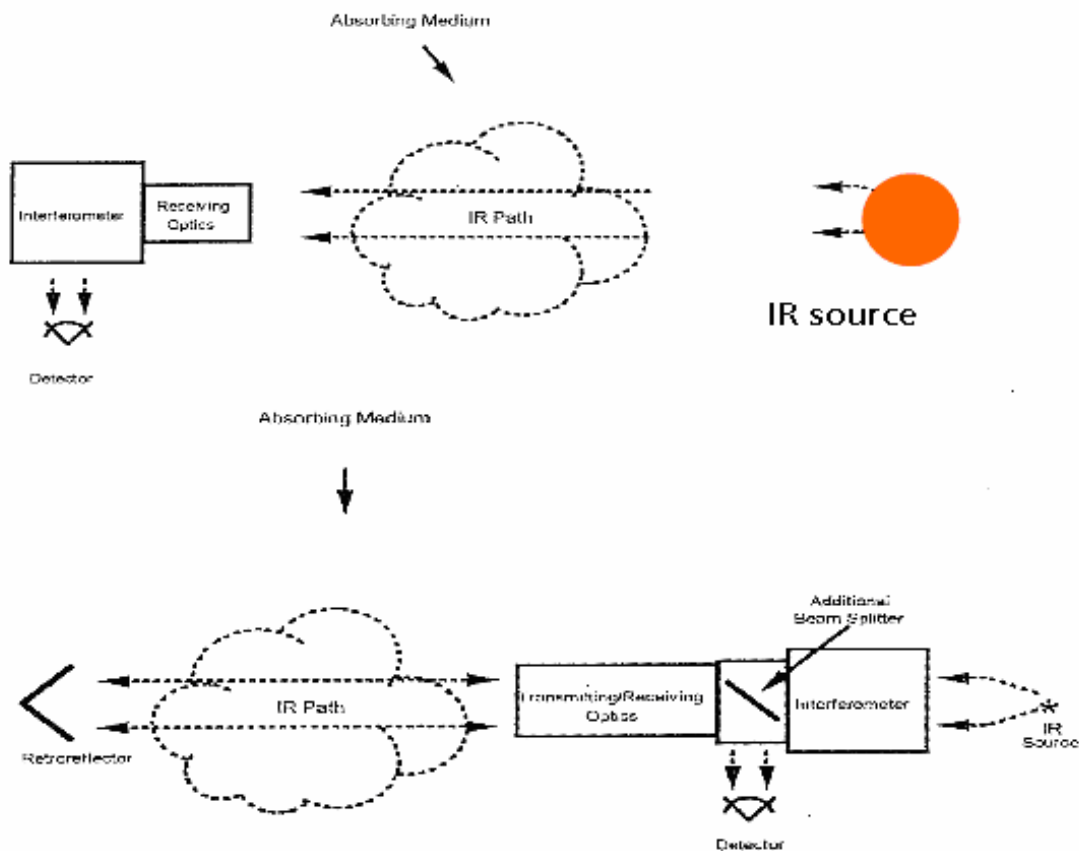


**Figure 1.** Active OP-FTIR configurations.

The quality of spectral data collected in the monostatic configuration is demonstrated in Figure 2. Three overlapping compounds are visible in a measurement campaign conducted in a Kentucky landfill where humidity was profound. The CLS analysis of the spectral region shown in Figure 2 yielded path-averaged concentrations of 761 ppb of ethanol, 814 ppb of ammonia and 49 ppb of methanol. Our newly developed real-time classical-least-square (CLS) software can identify the compounds, handle water interference, and minimize the incidence of false positives. Such quality analysis can be achieved only with the modulated active system. Still, at elevated temperature, non-modulated bistatic configuration OP-FTIR can perform much better than the passive FTIR both in detection levels and in occurrence of false positives.

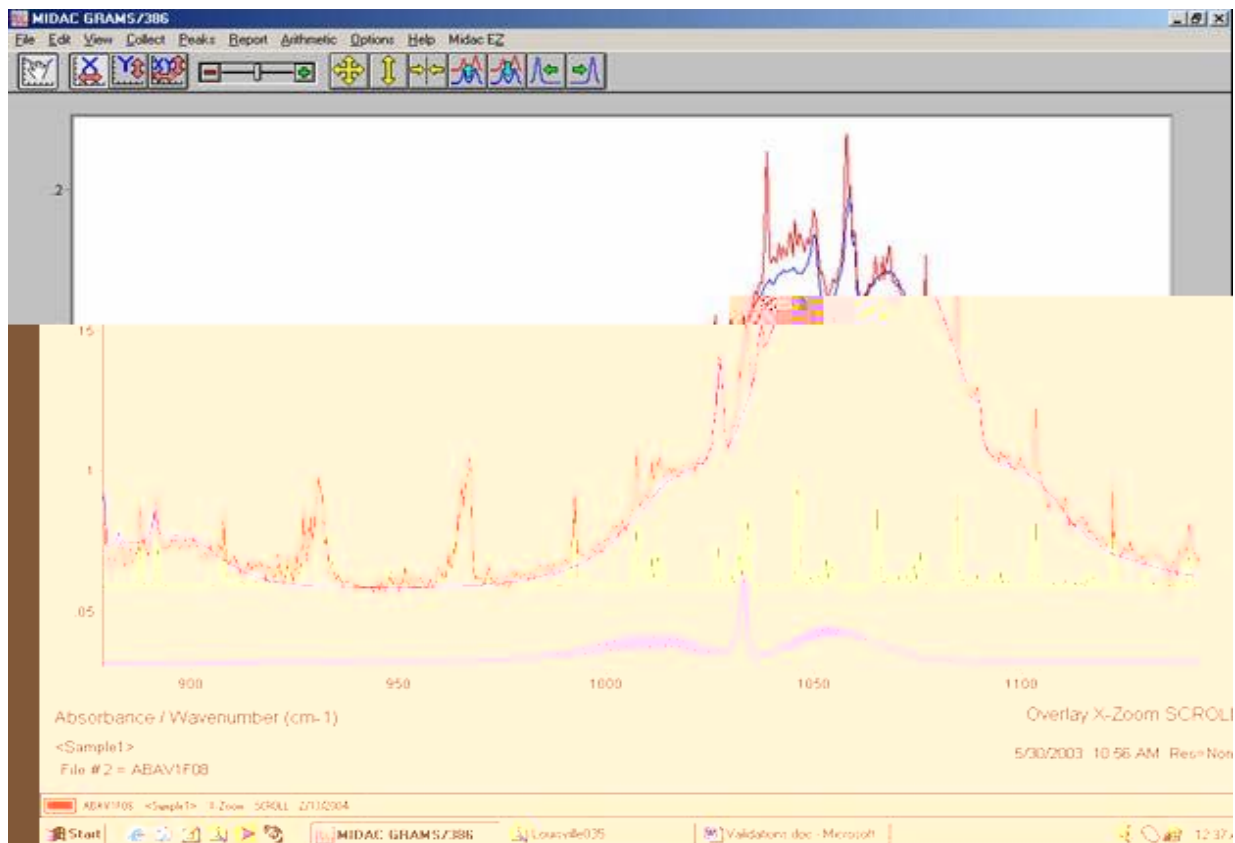


**Figure 2.** A field spectrum measured (red trace) and reference spectra of ethanol (blue trace), ammonia (green trace) and methanol (purple trace).

The EPA is considering using active OP-FTIR sensors (modulated and non-modulated) that utilize sources operating in the range of 300–1500 K. Our current hardware is an evolution of an OP-FTIR spectrometer originally developed for air quality monitoring of volatile organic compounds in the vapor phase. It uses a cooled mercury–cadmium telluride detector to accommodate the sensitivity requirements. In addition to furthering the development of the spectrometer hardware, we currently provide real-time software to identify CWA and TIC in both phases and with unprecedented sensitivity. Figure 3 provides an example of the EPA’s evaluation results. Sulfur hexafluoride detection levels were determined for a wide range of source temperatures from 4 to 300°C above ambient conditions for a non-modulated bistatic configuration. It is obvious from this example that as little as 70°C above ambient is sufficient to achieve a marked improvement in detection limit over the passive approach.

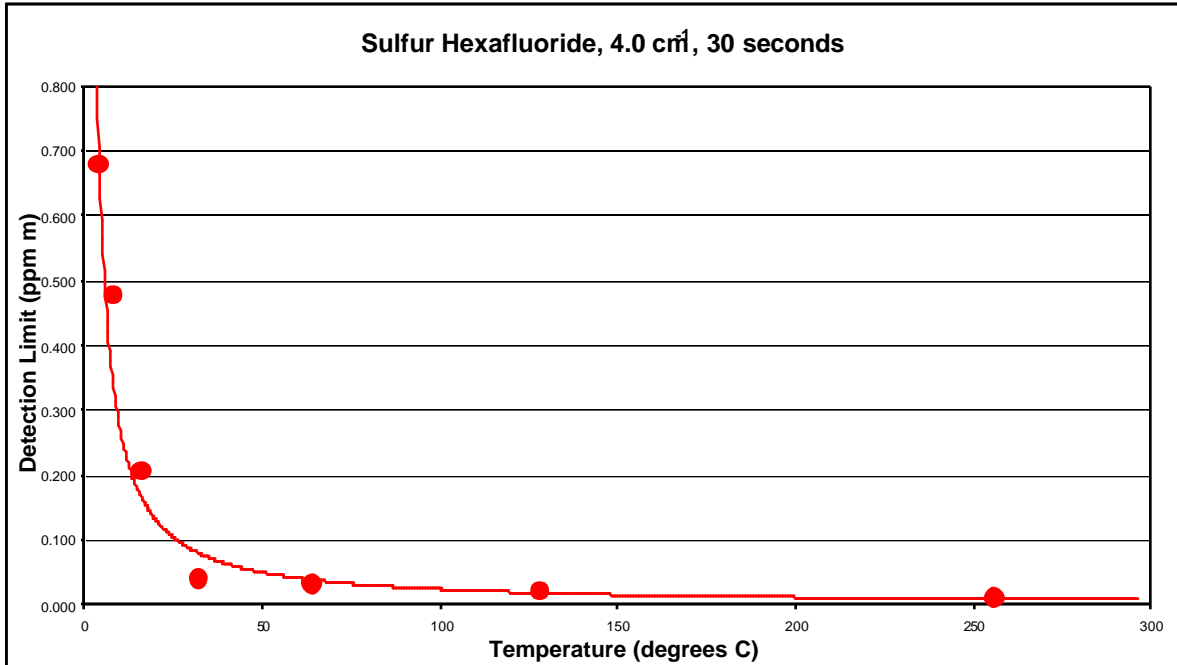


**Figure 3.** Active non-modulated OP-FTIR detection limits as a function of source temperature.

The high source temperature can provide more than 80-fold increase in the infrared radiant flux emitted per unit area in the 7–14- $\mu\text{m}$  spectral fingerprint region compared to passive FTIR. As a result, the active OP-FTIR sensors can detect CWAs such as GA, GB, GD, HD and Lewisite in the range of 1 to 10  $\mu\text{g}/\text{m}^3$ . These levels are orders of magnitude lower than those that passive systems are capable of detecting. Also with the progress being made in broad band quantum cascade (QC) laser technology, radiation sources for FTIR sensors are expected to improve significantly. This may allow waiving the use of expensive retroreflectors, and instead using natural or cheap manmade hard targets.

Figure 4 is a summary chart generated by the Army Chemical Materials Agency (CMA) to compare different sensors for CWAs detection. Originally, this chart accurately quoted detection limits of passive FTIR as used by the military. However, in some military operations active systems can be utilized for confirmation purposes and to protect personnel. The range of possible detection limits for an active OP-FTIR system was added to the CMA chart and is displayed as red bars.

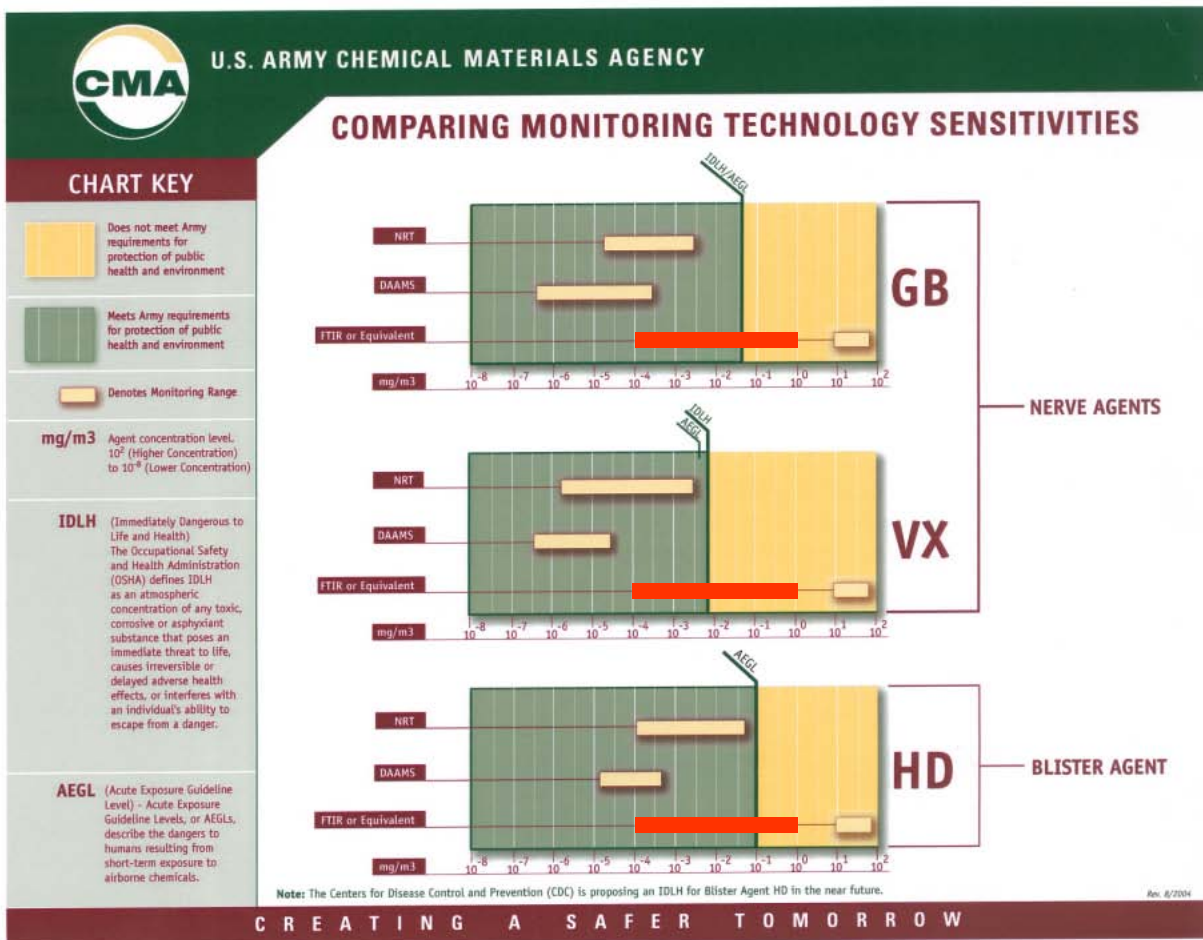


Figure 4. Army chemical material agency comparison among different sensors for CWAs detection.

The wide range of values depends on many measurement variables, such as source temperature, source modulation, type of detector, type of infrared source (QC lasers, yet to be developed, may provide unprecedented low detection limits), path length through the plume relative to the optical path length, atmospheric condition and more. Yet, for each specific measurement-and-system condition the detection limit can be accurately determined, screening out unwanted false positive readings. This will allow the users to enjoy the benefits of path integrated measurements, i.e., better capture of the entire plume, and still make use of several complementary sensitive point monitors for detection confirmation. These point monitors by themselves (without path-integrated data) may bias – most typically by underestimation of the extent of the plume – or worse, miss the entire plume. When multiple beams are scanned in different directions and path-lengths, the recently developed radial plume mapping (RPM) method can be applied to retrieve spatial gradients and profiles across the plume.

An OP-FTIR based RPM System, configured specifically to meet emergency response (ER) needs, has recently been purchased by North Carolina’s Department of Environment and Natural Resources (DENR), after it was pre-approved by the Department of Homeland Security. This ER-RPM system package included all instrumentation (Figure 5), computer hardware, and real-time RPM software necessary for rapid response and analysis of emergency situations. This

system can currently detect more than 100 TICs and CWAs, and has successfully passed a real-time acceptance test in which unknown gases were introduced to the beam path.



Figure 5. ER-RPM System, as sold to NC DEHNR

## 2. AEROSOL DETECTION AND IDENTIFICATION

In addition to the marked improvement in detection sensitivity, active sensors enjoy another very important advantage over the passive sensors; they can sensitively and reliably detect and identify aerosols. Low-vapor-pressure TICs, pesticides and CWAs may be released in aerosol form, and these aerosolized compounds exhibit characteristic and unique IR spectra, which can be measured and utilized for identification purposes. The following equation describes the IR light extinction by a particle–gas mixture as a function of wavelength:

$$A(\lambda) = S_e(\lambda) \cdot L + S_g(\lambda) \cdot CL \quad (1)$$

where,  $\bullet_g$  is the absorption coefficient of the gas ( $m^2/ppm$ ),  $L$  is the optical pathlength of the IR beam and  $C$  is the concentration (ppm). The wavelength-dependent extinction coefficient for the particles,  $\bullet_e$ , is given by:



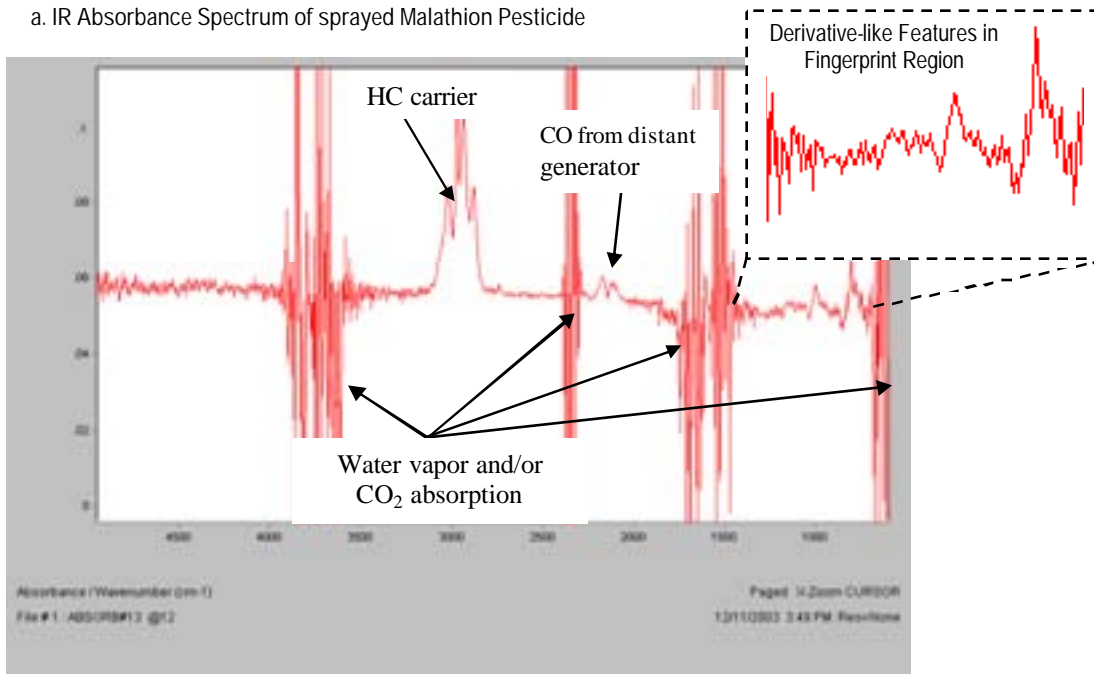
$$S_e(l) = \frac{\rho}{4} \sum_j Q_e(l)_j \cdot N_j \cdot d_j^2 \quad (2)$$

where,  $j$  denotes the particle size index,  $Q_e(\bullet)$  is the complex refractive index dependent extinction efficiency,  $N$  is the particle number density, and  $d$  is the particle diameter. At each wavelength, the contributions of all particle sizes add to produce the total extinction due to particles. The particles extinction contribution to the IR apparent absorbance spectrum can be computed by multiplying the extinction coefficient by  $L$ .

Figure 6a, which shows a measured absorbance spectrum of a particle–gas mixture, is intended to validate the above mathematical description. The field spectrum was measured using an IMAAC OP-FTIR (Figure 5) with a 70-m pathlength and a two-second integration time. A compressor and paint sprayer were used to aerosolize the compounds. The malathion pesticide was sprayed with equal volumes of the hydrocarbon carrier. The malathion pesticide is a low vapor pressure organophosphate similar to VX chemical agent both in its IR characteristics and in its volatility. A very small aerosol cloud was dispersed into the beam and the spectrum recorded. There are two aspects to figure 6a. The first is the wavelength-dependent baseline offset, which provides information about the presence of an aerosol plume in the optical beam. The slope of the baseline offset appears slightly negative in this spectrum because of the very fine aerosol mist. The very fine pesticide aerosol shows a stronger extinction contribution at the higher frequency (shorter wavelength) end of the spectrum (slightly negative slope). This pesticide employs a hydrocarbon carrier (exhibiting the  $3000 \text{ cm}^{-1}$  H–C stretch mode). The second, possibly more enlightening aspect is the derivative-like features in the  $700\text{--}1400 \text{ cm}^{-1}$  fingerprint regional. These are a result of the interdependence between the imaginary and real parts of the complex refractive index in the vicinity of an absorption feature of the aerosolized material.

We examined a malathion vapor-phase spectrum courtesy of NIST (Figure 6b) to demonstrate the lack of vapor-phase absorption features in the measured spectrum (low vapor pressure). It should be noted that a larger concentration would be expected for hazardous exposure levels, and we would expect to see spectral features due to vapor-phase absorption in addition to the aerosol features in this case. However, a very small amount of CO was measured from a distant generator. We also note that this technique can be used to determine the relationship between carrier and active ingredient concentrations for instances when the carrier is released alone.

a. IR Absorbance Spectrum of sprayed Malathion Pesticide



This pesticide employs an HC carrier (exhibiting the  $3000\text{ cm}^{-1}$  H-C stretch mode). Of particular relevance are the aerosol features in the fingerprint region ( $700$  to  $1400\text{ cm}^{-1}$ ), which illustrate the interdependence of the real and imaginary parts of the refractive index in the vicinity of an absorption feature (in the form of the derivative-like shaped features). We also note a baseline offset due to the aerosol scattering; the aerosol containing pesticide was very fine and shows a stronger extinction contribution at the higher-frequency (shorter wavelength) end of the spectrum (slightly negative slope).

b. IR Absorbance Spectrum of Vapor-phase Malathion Pesticide

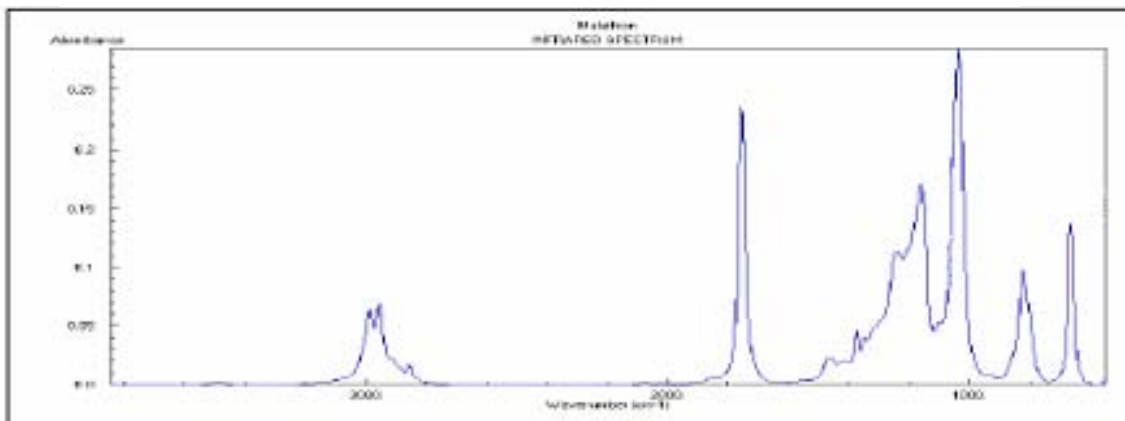


**Figure 6.** Aerosolized malathion pesticide field spectrum (a) along with a reference spectrum of malathion vapor (b).

Similar derivative-shaped features are expected for low-vapor-pressure chemical agents such as VX. In a simulation performed by Flanigan (1985) the transmission of a pure  $5\text{-}\mu\text{m}$  mono-disperse VX aerosol was calculated for the  $8\text{--}13\text{ }\mu\text{m}$  spectral region. The main derivative feature of the VX between  $9\text{--}10\text{ }\mu\text{m}$  is very similar to the measured malathion feature. Assuming similar optical absorption and density properties for the two compounds, the minimum detection level for VX over a  $200\text{-m}$  pathlength is estimated to be roughly  $50\mu\text{g}/\text{m}^3$  in the liquid phase,

with a time resolution of 2 seconds. In such concentration we do not expect to see any gas-phase features. However, in more acute exposure levels the gas phase may be detected, and support the definitive identification of the chemical agent. These types of very sensitive identification capabilities are feasible only with monostatic, stable, modulated OP-FTIR system.

It is expected that different compounds will have unique signatures. The width of the features will vary slightly with changes in aerosol size. Absorption by aerosol material (liquid or solid), as expressed by the imaginary part of the complex refractive index, will occur at particular wavelengths for different aerosol material, typically in the fingerprint region. In the extinction spectrum of a suspended aerosol cloud this absorption will usually be represented by a derivative-like shear of the spectrum baseline if size-dependent scattering occurs in the region. If particles are very small or several absorption lines are adjacent to each other, the absorption feature in the extinction spectrum may look similar to typical gas absorption features (Lorentzian). Regardless of the shape, the magnitude of the absorption feature must correlate perfectly with the scattering baseline offset as both phenomena represent the presence of an aerosol cloud. In a simulation performed by our research team, VX aerosol extinction spectrum was calculated for the  $950\text{--}1100\text{ cm}^{-1}$  ( $9.1\text{--}10.5\text{ }\mu\text{m}$ ) spectral region, using the known complex refractive index spectrum of VX in this spectral region (Figure 7). This is compared to the spectrum of the small amount of aerosolized malathion. Derivative-like features of the VX spectrum are similar to the measured malathion features also shown in Figure 7.

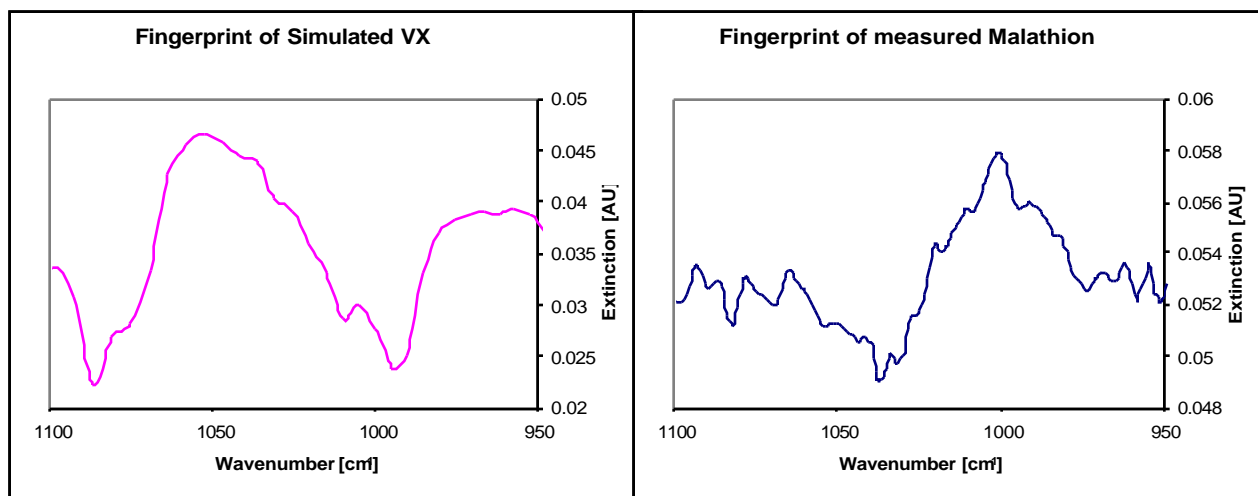


**Figure 7.** Simulated VX features compared with measured malathion features.

It is noted that for VX, there are two derivative-like features in the  $1100\text{--}950\text{ cm}^{-1}$  region, whereas for malathion there is one between  $1040\text{--}1000\text{ cm}^{-1}$ . The rising side of the feature (or shear) is specific to one type of aerosol in the specific spectral region in which it appears. Since VX has two of these features in this region, the probability of detection and identification is very high with minimal likelihood of false positive identification. The specific region of the shear is independent of size distribution for a large range of mean aerosol size, although the baseline offset and feature's shape may vary with the amount of aerosol and the size distribution of particles present in the optical beam. Like VX, malathion is an organophosphate with similarly low vapor pressure ( $4\times 10^{-5}$  torr for malathion at  $25^{\circ}\text{C}$  and  $6\times 10^{-4}$  torr at  $25^{\circ}\text{C}$  for VX). Figure 8 shows the simulation of the VX features using the Mie theory for a normal distribution of aerosol

sizes with three different scenarios of mean (2–10  $\mu\text{m}$ ) particle diameter and standard deviation. This Figure shows that the features mentioned above can be used for successful identification of VX from spectra acquired in the IR region of 1100–950  $\text{cm}^{-1}$  (9.1–10.5  $\mu\text{m}$ ). The research team has performed simulations of many more scenarios, including monodisperse VX aerosol, all of which lead to the same conclusion.

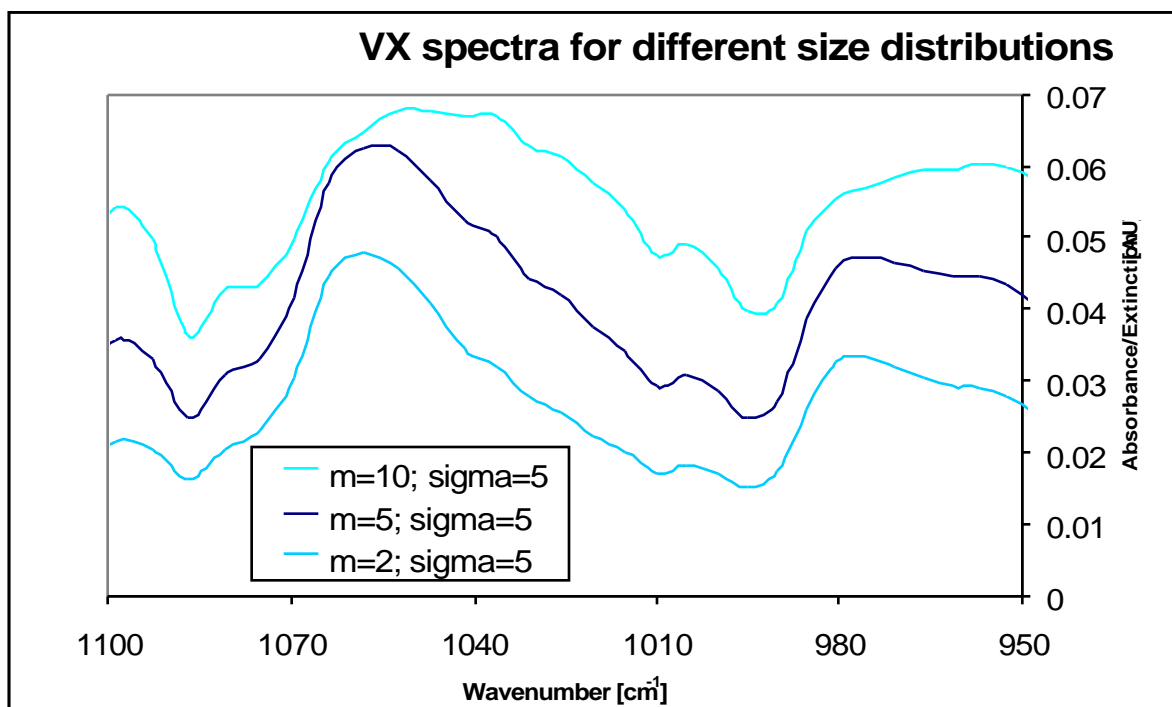


**Figure 8.** VX Spectral features for three different aerosol size distributions.

The research team has extensive experience in identifying several particulate materials that can introduce false positive detection in the battle field. While a specific dust feature may overlap one of the shear features of VX, the probability of having both shear features overlapped by any other aerosol in the same ratio is very remote.

## CONCLUSION

This paper emphasizes the superiority of the active OP-FTIR systems over the passive systems in detection levels and data quality. Moreover, it disputes the misconceptions that are generally accepted for FTIR technologies. Our broader research team (EPA, ARCADIS, AFRL, and other federal, academic, and private organizations) includes many scientists with extensive experience (each between 15 and 25 years) in optical remote sensing (ORS) techniques both for particulate and gas phase measurements. ARCADIS is the long-term onsite contractor for EPA/ORD and was intimately involved in all the ORS research conducted by the EPA in the last five years. Additionally, in the last three years ARCADIS ORS group has been contracted by the Air Force (AFRL) and Army (CERL) to perform ORS research and development. As a result of these collaborations, four projects funded by the DoD Strategic Environmental Research and Development

Program (SERDP) applying ORS techniques have materialized. In all of these activities, new approaches for detection and identification of aerosolized and vaporized threats using an active modulated OP-FTIR have been developed. Our research team is always in favor of combining ORS and more conventional methods to enhance and improve detection and identification capabilities. In light of these developments, revisiting a detection approach that includes active OP-FTIR system is strongly recommended as many non-battlefield detection applications have recently emerged.

## REFERENCES

1. R.A. Hashmonay and M.G. Yost, "On the Application of OP-FTIR Spectroscopy to Measure Aerosols: Observations of Water Droplets", *ES&T*, 33(7), 1141–1144, April 1999.
2. *Analytical Chemistry News & Features*, June 1 1999, 371 A
3. Flanigan D., The Spectral Signatures of Chemical Agents Vapors and Aerosols, Chemical Research and Development Center, CRDC-TR-85002, 1985.
4. R. Hashmonay, A. Cohen and U. Dayan, "LIDAR Observations of the Atmospheric Boundary Layer in Jerusalem", *J. Appl. Meteor.*, 30, 1228–1236 (1991).
5. R.A. Hashmonay, D.F. Natschke, K. Wagoner, D. B. Harris and E.L. Thompson, "Field Evaluation of a Method for Estimating Gaseous Fluxes from Area Sources Using Open-Path Fourier Transform Infrared", *ES&T*, 35(11), June 2001, 2309–2313.
6. M.Y. Tsai, M.G. Yost, C.F. Wu, R.A. Hashmonay, and T.V. Larson, "Line Profile Reconstruction: Validation and Comparison of Reconstruction Methods", *Atmospheric Environment*, 35(28), 4791–4799, 2001.
7. R.A. Hashmonay, M.G. Yost and Chang-Fu Wu, "Computed Tomography of Air Pollutants Using Radial Scanning Path-Integrated Optical Remote Sensing", *Atmospheric Environment*, 33(2), 267–274 (1999).
8. R.A. Hashmonay and M.G. Yost, "Innovative Approach for Estimating Gaseous Fugitive Fluxes Using Computed Tomography and Remote Optical Sensing Techniques", *JA&WMA*, 49, 966–972, Aug. 1999.
9. R.A. Hashmonay and M.G. Yost, "Localizing Gaseous Fugitive Emission Sources by Combining Real Time Optical Remote Sensing and Wind Data", *JA&WMA*, 49, 1374–1379, Nov. 1999.
10. Wu, C.F., Yost M.G., Hashmonay, R.A., Park D.Y., "Experimental Evaluation of a Radial Beam Geometry for Mapping Air Pollutants Using Optical Remote Sensing and Computed Tomography", *Atmospheric Environment*, 33(28), 4709–4716 (1999).

11. Gmachl et al., *Nature*, **415**, 883-887